Supplementary Information Appendix for Low risk of SARS-CoV-2 transmission via fomite, even in cold-chain.

Author names and affiliations: Julia S. Sobolik, MS[a1], Elizabeth T. Sajewski, MS[a], Lee-Ann Jaykus, PhD[b], D. Kane Cooper, MSPH[a], Ben A. Lopman, PhD[a], Alicia NM. Kraay, PhD[a], P. Barry Ryan, PhD[a], Jodie L. Guest, PhD[a], Amy Webb-Girard, PhD[a], Juan S. Leon, PhD[a]

[1]Rollins School of Public Health, Emory University, Atlanta, GA USA

[2]Food, Bioprocessing and Nutrition Sciences, North Carolina State University, Raleigh, NC, 27695

* Corresponding author: Julia S. Sobolik; email: julia.sobolik@emory.edu

Supplementary Information Appendix

Materials and methods:

Model conceptualization and vetting

Model design was informed by several frozen fruit and vegetable manufacturers and their trade association, the American Frozen Food Institute. Following initial development, the model was vetted by food industry experts: Dr. Sanjay Gummalla [Senior Vice President, Scientific and Regulatory Affairs, American Frozen Food Institute] and Dr. Lory Reveil [Director, Scientific and Regulatory Affairs, American Frozen Food Institute].

Data sources

The model assumed two infected workers (as unvaccinated or as rare breakthrough infections) and that the infected and susceptible workers were independent of one another. To calculate viral shedding of the infected workers, we converted PCR-based genome equivalent copies to PFU using a 1:100 conversion, as previously applied by Pitol *et al*.[1] This resulted in SARS-CoV-2 titers in saliva (range: 6·1 to 7·4 $\log_{10}$ PFU/mL),[2,3] representative of peak virus titer reported around the time of symptom onset [3,4] and the acute phase of infection, when the majority of transmission events are thought to occur.[4,5] The same distribution of shedding data was used for both infected workers. To determine the amount of virus expelled into the air by the infected workers, the total fraction of saliva volume released during coughing was calculated for each droplet (50-60µm, 60-100µm, >100µm) and aerosol (<50µm) range as described in [6] using respiratory particle counts and size distributions from empirical studies.[7]

The model simulated equal probability of cough events for each infected worker, ranging from 0-10 coughs, over the duration of product packaging (1h-period). Aerosol transport properties of the differently-sized respiratory particles informed the contamination potential of the plastic packaging. For instance, aerosols defined as <50 µm in diameter settle from the air according to their terminal settling velocity. Droplets (50-750 µm) fall rapidly due to gravitational forces and their ability to contaminate fomites as fallout or spray was determined by size and distance traveled based on modeling studies.[8] The proportion of droplets that reached the plastic cartons or plastic wrap within 0 to 3 feet distancing was derived from modeling studies by.[8]

Viral decay [9] was included at two stages in the model: 1) virus-containing aerosols or droplets in the air; and 2) the virus-contaminated hands of the susceptible worker. The model assumed no viral decay during pallet transport, holding, and unpacking while under cold chain storage conditions.[9-12] Additionally, the model assumed the susceptible worker had no additional SARS-CoV-2 exposures in the receiving warehouse (e.g., local community transmission, other infected workers in the receiving warehouse etc.,). Given heterogeneity in the volume of products processed over a contiguous workday, a 1-hour period was modeled to more precisely represent the number of products handled by workers within under cold-chain conditions. Further, the model exclusively simulated fomite-mediated transmission and did not capture potential respiratory exposures associated with re-aerosolization of virus particles from fomites. Virus transfer efficiencies from

plastic fomite surfaces (individual plastic cartons, palletized cartons, plastic wrap) to hands leveraged laboratory-based studies using acrylic surfaces under low-humidity conditions and the viral surrogate MS2.[13] Sequential tactile events were modeled from the initial contact of the susceptible worker's hand to the fomite surface (one contact/individual plastic carton; up to 20 contacts on the pallet plastic wrap) followed by hand contact to facial mucous membranes (0·8 contacts/minute).[14] SARS-CoV-2 infection risks were estimated using an exponential dose-response model based on the pooled data from studies of SARS-CoV and murine hepatitis virus infection in mice by intranasal administration [15,16] with the ID_{50} equal to 102 infectious particles. We applied this SARS-CoV dose-response model given the high degree of comparability to SARS-CoV-2 (e.g., genetic and amino acid homology, transmission pathways, etc.).[17]

Infection control measures were implemented to reduce contamination of the plastic packaging (i.e., mask use by the infected workers) or to disrupt the transfer of virus from the susceptible worker's hands to their mucous membranes (handwashing). Laboratory-based studies on mask filtration efficiencies [18-21] were used to inform estimates of surgical masking efficacy. Using these empirical studies, which reported mask filtration efficiencies for either source control and/or recipient protection, we calculated the mask efficacy for when the infected workers wore the mask (source) and for when the susceptible worker (recipient) wore the mask. Of note, we assumed no reduction in hand to face contacts when the susceptible worker was contacting their face. Handwashing and package surface disinfection virus removal efficiencies were representative of current CDC and EPA List N: Disinfectants for Coronavirus (COVID-19) products: handwashing (2 $\log_{10}$ virus removal);[22] and plastic packaging decontamination (3 $\log_{10}$ virus removal).[23] For all mitigation strategies (mask use, handwashing, and surface decontamination), we assumed that these were implemented with 100% compliance and in the specified manner. A routine ventilation rate was applied across all modeled scenarios defined as two complete room air changes per hour (ACH).

Vaccination was incorporated into the model representing two doses of mRNA vaccine (Moderna/Pfizer) and was applied with and without the standard infection control measures. For the first vaccination scenario, we assumed only the susceptible worker was vaccinated with two doses of mRNA vaccine (Moderna/Pfizer) and vaccine effectiveness (VE) against susceptibility to infection was simulated across three vaccination states. These included: 1) no vaccination/no prior immunity; 2) lower VE ranging from 64[24]-80%[25] representative of reduced protection (variants of concern, waning immunity, immunocompromised and elderly or at-risk populations); and 3) optimal VE ranging from 86%[26,27]-99[28]% among healthy adults 14 days or more after second mRNA dose. The second vaccine scenario represented vaccine effectiveness against transmission, where all workers are assumed to vaccinated with two doses of the mRNA vaccines and hence the model simulated rare breakthrough infections. Vaccine effectiveness against transmission (VET) was modeled by applying the combined effect of the reduction in risk of infection to the susceptible worker and the risk of transmissibility given a rare breakthrough infection among the vaccinated workers. We used the VET estimate (88·5% [95%CI: 82·3%, 94·8%] derived from Prunas *et al.,*[29] VET was modeled across a range of three peak infectious viral shedding concentrations representative of possible increased transmissibility and/or infectiousness of variants of concern: 1) 8·1-9·4 $\log_{10}$ viral particles; 2) 7·1-8·4 $\log_{10}$ viral particles; and 3) 6·4-7·7 $\log_{10}$ viral particles. These viral shedding levels are 100-, 10-, and 2-times, respectively, the increased viral shedding concentration simulated in the base model analysis. For all vaccination scenarios, VE was applied directly to the model-derived risk estimates to represent reduction in infection risk. An assumption of this model is that VE would have the same impact across transmission pathways (aerosol, droplet, and fomite-mediated).

Model parameters associated with the indoor facility and respiratory transmission (aerosols and droplets) modes were described in.[30] However, air temperature was modified from 70 to 55°C to represent ambient air temperatures used during the process of freezing and packaging frozen foods. In addition, extensive sensitivity analyses including the number of simulations needed to achieve model stability; variability and uncertainty propagation throughout the model; and identifying the most influential parameters for SARS-CoV-2 infection risk, reported as Spearman's correlation coefficients, were previously described in Sobolik *et al.*[30]

Results:

Impact of infection control measures on fomite-mediated SARS-CoV-2 infection risks with variants of concern from breakthrough cases

Increased viral shedding (8·1-9·4 $\log_{10}$ infectious virus [100X baseline shedding concentration]) resulted in an infection risk of 2·8 x 10^{-2} per 1h-period (95%CI: 7·8 x 10^{-5}, 1·1 x 10^{-1}) (Figure 2B). Implementing standard infection control measures reduced risk to near the 10^{-4} risk threshold: by 98·9% for handwashing (3·2 x 10^{-4} risk per 1h-period, 95%CI: 7·8 x 10^{-7}, 2·7 x 10^{-3}) and by 99·6% for handwashing and masks (1·1 x 10^{-4} risk per 1h-period, 95%CI: 2·6 x 10^{-7}, 9·4 x 10^{-4}), relative to no infection control measures.

Estimated SARS-CoV-2 concentration on combined plastic packaging under cold-chain conditions

SARS-CoV-2 concentration on combined plastic packaging in the absence of infection control measures was 11·7 infectious viruses/m^2 (95%CI: 2·6 x 10^{-2}, 6·9 x 10^{1}) (*SI Appendix*, Figure S1.A). Mask use led to a 66·7% reduction in SARS-2 concentration on fomites. The addition of plastic packaging decontamination resulted in 3·5 $\log_{10}$ reduction (3·9 x 10^{-3} infectious viruses/m^2 [95%CI: 8·8 x 10^{-6}, 2·3 x 10^{-2}]). Handwashing by the infected workers had no impact on the fomite SARS-CoV-2 concentration as this exposure route was not considered.

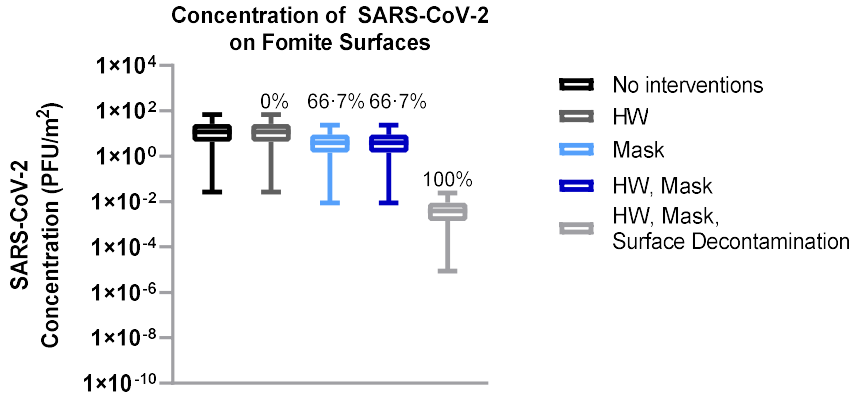

Fig. S1. Concentration of SARS-CoV-2 on combined fomites (individual plastic cartons, plastic wrap). SARS-CoV-2 concentrations on plastic fomite surfaces associated with standard SARS-CoV-2 infection control measures (hourly handwashing, universal surgical mask usage) under cold-chain conditions. Ventilation (two air changes per hour [ACH]) was assumed for all simulations. Percent reduction reported above each boxplot relative to no interventions.

Table S1. Model parameter inputs and distributions.

Parameter	Units	Description	Distribution	Input Values	Citations
Viral shedding					
$Log_{10}(C_{virus})$	PFU/mL	Concentration of virus in saliva 100X increased viral shedding 10X increased viral shedding 2X increased viral shedding	Triangular	6·8 (6·1, 7·4) 8·8 (8·1, 9·4) 7·8 (7·1, 8·4) 7·1 (6·4, 7·7)	[2,3]
$V_{F,c}$	mL/Cough	Fraction of volume associated with aerosols (2–45μm)	Triangular	$2{\cdot}3 \times 10^{-6}$ ($1{\cdot}4 \times 10^{-6}$, $2{\cdot}6 \times 10^{-6}$)	[7]
$V_{F,c}$	mL/Cough	Fraction of volume associated with droplets (50–60μm)	Triangular	$6{\cdot}0 \times 10^{-6}$ ($3{\cdot}5 \times 10^{-6}$, $6{\cdot}7 \times 10^{-6}$)	[7]
$V_{F,c}$	mL/Cough	Fraction of volume associated with droplets (60–100μm)	Triangular	$4{\cdot}9 \times 10^{-6}$ ($1{\cdot}1 \times 10^{-6}$, $8{\cdot}4 \times 10^{-6}$)	[7]
$V_{F,c}$	mL/Cough	Fraction of volume associated with droplets (100–750μm)	Triangular	$6{\cdot}8 \times 10^{-3}$ ($4{\cdot}0 \times 10^{-3}$, $7{\cdot}6 \times 10^{-3}$)	[7]
F_C	Cough/h	Number of coughs per hour	Empirical	1/11 equal probability (0, 10)	[31,32]
λ_{virus}	Hour	Viral decay of SARS-CoV-2 at 40% relative humidity, 55°F	Point value	0·1447	[33]
pp	Probability	Probability respiratory particles will remain in the air as respiratory spray between 0 and 1m distancing	Uniform	50-60μm: 1m: 0·82; 60-100μm: 1m: 0·44; >100μm: 1m: 0·04	[8]
$pp_{droplets}$	Probability	Probability respiratory particles (>100 μm) will remain in the air as respiratory spray between 0 and 1m distancing	Uniform	(0·01, 0·22)	[8]
$pp_{falldroplets}$	Probability	Probability respiratory particles (>100 μm) will settle to the fomite surfaces between 0 and 1m distancing	Uniform	(0·07, 0·78)	[8]
Risk mitigation interventions[1]					
S_{mask}	Log reduction	Source protection surgical mask efficacy	Uniform	(0·39, 0·57)	[20,34,35]
RS_{mask}	Percent reduction	Recipient surgical mask efficacy	Uniform	(0·37, 0·998)	[20,34,35]
SD_{eff}	Log reduction	Plastic fomite surface decontamination efficiency	Point value	$3Log_{10}$ virus	[23,36]
HW_{eff}	Log reduction	Handwashing efficiency	Point value	$2Log_{10}$ virus	[37,38]
HW_{freq}	Handwashing/h	Frequency of handwashing per hour	Point value	1·0	Expert elicitation
R_{air}	Air changes/h	Frequency of room air changes per hour (ACH)	Point value	ACH 2	Expert elicitation
$VE_{optimal}$	Percent reduction	Vaccine effectiveness	Uniform	(0 ·86,0·99)	[26-28]
$VE_{reduced}$	Percent reduction	Vaccine effectiveness	Uniform	(0·64,0·80)	[24,25]
VET	Percent reduction	Vaccine effectiveness against transmission	Triangular	0·89(0·82,0·95)	[29]
Fomite-mediated transmission					
$SA_{carton.top}$	m^2	Surface area of top of individual plastic carton	Uniform	(0·106, 0·116)	Assumed
SA_{carton}	m^2	Surface area of a single individual plastic carton	Uniform	(0·41, 0·54)	Assumed
Cartons	Cartons/h	Number of individual plastic cartons processed per h	Uniform	(144, 216)	Assumed

Pallets	Pallets/h	Number of pallets processed per h	Point value	4	Assumed
$SA_{plasticwrap.side}$	m^2	Surface area of a single side of plastic wrapped pallet	Uniform	(4·2, 6·97)	Assumed
$SA_{plasticwrap}$	m^2	Surface area of entire plastic wrapped pallet	Uniform	(25·2, 41·8)	Assumed
$Fingers_{sa}$	m^2	Surface area of three finger tips touching the surface	Point value	0·00042	[39]
H_{sa}	m^2	Area of two hands (palms only)	Point value	0·049	[39]
F_{decay}	Hour	Viral decay rate (PFU per hour)	Point value	0·15	[9]
TE_{fh}	PFU	Viral transfer fraction from fomite to hand with relative humidity (40-65%); acrylic surface	Normal	0·795 (0·212)	[13]
TE_{hf}	PFU	Viral transfer fraction from hand to fomite surface	Point value	0·025	[40-43]
TE_{hm}	PFU	Viral transfer fraction from hand to face	Normal	0·20 (0·063)	[13]
freq.hs	Contacts/min	Frequency of contacts from hand to individual plastic cartons	Point value	Cartons/60	Assumed
freq.hs.pw	Contacts/min	Frequency of contacts from hand to plastic wrap	Uniform	(4/60, 20/60)	Assumed
freq.hf	Contacts/min	Frequency of contacts from hand to face	Point value	0 ·8	[14]
$Hand_{decay}$	Minutes	Viral decay rate on hands (PFU/min)	Uniform	(0·92, 1·47)	[41]
eyes.sa	m^2	Surface area of mucous membranes—eyes	Uniform	($1x10^{-5}$, $2x10^{-4}$)	[44]
nose.sa	m^2	Surface area of mucous membranes—nose	Uniform	($1x10^{-5}$, $1x10^{-3}$)	[44]
mouth.sa	m^2	Surface area of mucous membranes—mouth	Uniform	($1x10^{-4}$, $4.1x10^{-3}$)	[44]
SARS-CoV-2 dose and risk characterization					
$Ratio_{infectious}$	No units	Infectious to non-infectious ratio	Point value	1:100	[45]
k_{risk}	PFU^{-1}	Dose-response parameter	Point value	0·00680	[1]

[1]All interventions were assumed to be implemented with 100% compliance.

SI References

1. Pitol AK, Julian TR. Community Transmission of SARS-CoV-2 by Surfaces: Risks and Risk Reduction Strategies. *Environ Sci Technol Lett*. 2021.
2. To KK-W, Tsang OT-Y, Yip CC-Y, Chan K-H, Wu T-C, Chan JM-C, et al. Consistent Detection of 2019 Novel Coronavirus in Saliva. *Clin Infect Dis*. 2020;**71**(15):841-3.
3. Wolfel R, Corman VM, Guggemos W, Seilmaier M, Zange S, Muller MA, et al. Virological assessment of hospitalized patients with COVID-2019. *Nature*. 2020;**581**(7809):465-9.
4. He X, Lau EHY, Wu P, Deng X, Wang J, Hao X, et al. Temporal dynamics in viral shedding and transmissibility of COVID-19. *Nat Med*. 2020;**26**(5):672-5.
5. Tian L, Li X, Qi F, Tang Q-Y, Tang V, Liu J, et al. Harnessing peak transmission around symptom onset for non-pharmaceutical intervention and containment of the COVID-19 pandemic. *Nat Commun*. 2021;**12**(1):1147.
6. Nicas M, Nazaroff WW, Hubbard A. Toward understanding the risk of secondary airborne infection: emission of respirable pathogens. *J Occup Environ Hyg*. 2005;**2**(3):143-54.
7. Chao CYH, Wan MP, Morawska L, Johnson GR, Ristovski ZD, Hargreaves M, et al. Characterization of expiration air jets and droplet size distributions immediately at the mouth opening. *J Aerosol Sci*. 2009;**40**(2):122-33.
8. Bourouiba L, Dehandschoewercker E, Bush JWM. Violent expiratory events: On coughing and sneezing. *J Fluid Mech*. 2014;**745**:537-63.
9. van Doremalen N, Bushmaker T, Morris DH, Holbrook MG, Gamble A, Williamson BN, et al. Aerosol and Surface Stability of SARS-CoV-2 as Compared with SARS-CoV-1. *N Engl J Med*. 2020;**382**(16):1564-7.
10. Riddell S, Goldie S, Hill A, Eagles D, Drew TW. The effect of temperature on persistence of SARS-CoV-2 on common surfaces. *Virol J*. 2020;**17**(1):145.
11. Pastorino B, Touret F, Gilles M, de Lamballerie X, Charrel RN. Prolonged Infectivity of SARS-CoV-2 in Fomites. *Emerg Infect Dis*. 2020;**26**(9).
12. Paton S, Spencer A, Garratt I, Thompson KA, Dinesh I, Aranega-Bou P, et al. Persistence of SARS-CoV-2 virus and viral RNA in relation to surface type and contamination concentration. *Appl Environ Microbiol*. 2021.
13. Lopez GU, Gerba CP, Tamimi AH, Kitajima M, Maxwell SL, Rose JB. Transfer efficiency of bacteria and viruses from porous and nonporous fomites to fingers under different relative humidity conditions. *Appl Environ Microbiol*. 2013;**79**(18):5728-34.
14. Nicas M, Best D. A study quantifying the hand-to-face contact rate and its potential application to predicting respiratory tract infection. *J Occup Environ Hyg*. 2008;**5**(6):347-52.
15. De Albuquerque N, Baig E, Ma X, Zhang J, He W, Rowe A, et al. Murine hepatitis virus strain 1 produces a clinically relevant model of severe acute respiratory syndrome in A/J mice. *J Virol*. 2006;**80**(21):10382-94.
16. Dediego ML, Pewe L, Alvarez E, Rejas MT, Perlman S, Enjuanes L. Pathogenicity of severe acute respiratory coronavirus deletion mutants in hACE-2 transgenic mice. *Virology*. 2008;**376**(2):379-89.
17. Hu B, Guo H, Zhou P, Shi Z-L. Characteristics of SARS-CoV-2 and COVID-19. *Nat Rev Microbiol*. 2021;**19**(3):141-54.
18. Asadi S, Cappa CD, Barreda S, Wexler AS, Bouvier NM, Ristenpart WD. Efficacy of masks and face coverings in controlling outward aerosol particle emission from expiratory activities. *Sci Rep*. 2020;**10**(1):15665.
19. Fischer EP, Fischer MC, Grass D, Henrion I, Warren WS, Westman E. Low-cost measurement of face mask efficacy for filtering expelled droplets during speech. *Sci Adv*. 2020;**6**(36).
20. Lindsley WG, Blachere FM, Law BF, Beezhold DH, Noti JD. Efficacy of face masks, neck gaiters and face shields for reducing the expulsion of simulated cough-generated aerosols. *Aerosol Sci Tech*. 2020:1-9.
21. Pan J, Harb C, Leng W, Marr LC. Inward and outward effectiveness of cloth masks, a surgical mask, and a face shield. *medRxiv*. 2020:2020.11.18.20233353.
22. Grove SF, Suriyanarayanan A, Puli B, Zhao H, Li M, Li D, et al. Norovirus cross-contamination during preparation of fresh produce. *International Journal of Food Microbiology*. 2015;**198**:43-9.
23. United States Environmental Protection A. List N: Disinfectants for Coronavirus (COVID-19). *Pesticide Registration*. 2020:2020-.

24. Moustsen-Helms IR, Emborg H-D, Nielsen J, Nielsen KF, Krause TG, Mølbak K, et al. Vaccine effectiveness after 1st and 2nd dose of the BNT162b2 mRNA Covid-19 Vaccine in long-term care facility residents and healthcare workers – a Danish cohort study *medRxiv*. 2021:2021.03.08.21252200.
25. Khan N, Mahmud N. Effectiveness of SARS-CoV-2 Vaccination in a Veterans Affairs Cohort of Patients With Inflammatory Bowel Disease With Diverse Exposure to Immunosuppressive Medications. *Gastroenterology*. 2021.
26. Andrejko KL, Pry J, Myers JF, Jewell NP, Openshaw J, Watt J, et al. Prevention of COVID-19 by mRNA-based vaccines within the general population of California. *medRxiv*. 2021:2021.04.08.21255135.
27. Pawlowski C, Lenehan P, Puranik A, Agarwal V, Venkatakrishnan AJ, Niesen MJM, et al. FDA-authorized mRNA COVID-19 vaccines are effective per real-world evidence synthesized across a multi-state health system. *Med (N Y)*. 2021.
28. Swift MD, Breeher LE, Tande AJ, Tommaso CP, Hainy CM, Chu H, et al. Effectiveness of mRNA COVID-19 vaccines against SARS-CoV-2 infection in a cohort of healthcare personnel. *Clin Infect Dis*. 2021.
29. Prunas O, Warren JL, Crawford FW, Gazit S, Patalon T, Weinberger DM, et al. Vaccination with BNT162b2 reduces transmission of SARS-CoV-2 to household contacts in Israel. *medRxiv*. 2021:2021.07.13.21260393.
30. Sobolik JS, Sajewski ET, Jaykus L-A, Cooper DK, Lopman BA, Kraay ANM, et al. Controlling risk of SARS-CoV-2 infection in essential workers of enclosed food manufacturing facilities. *medRxiv*. 2021:2021.05.14.21257244.
31. Adhikari U, Chabrelie A, Weir M, Boehnke K, McKenzie E, Ikner L, et al. A Case Study Evaluating the Risk of Infection from Middle Eastern Respiratory Syndrome Coronavirus (MERS-CoV) in a Hospital Setting Through Bioaerosols. *Risk Analysis*. 2019;**39**(12):2608-24.
32. Loudon RG, Roberts RM. Droplet expulsion from the respiratory tract. *Am Rev Respir Dis*. 1967;**95**(3):435-42.
33. Estimated Airborne Decay of SARS-CoV-2 (virus that causes COVID-19) under a range of temperatures, relative humidity, and UV index. In: Security DoH, editor. 2021.
34. Ueki H, Furusawa Y, Iwatsuki-Horimoto K, Imai M, Kabata H, Nishimura H, et al. Effectiveness of Face Masks in Preventing Airborne Transmission of SARS-CoV-2. *mSphere*. 2020;**5**(5):e00637-20.
35. Maurer L, Peris D, Kerl J, Guenther F, Koehler D, Dellweg D. Community Masks During the SARS-CoV-2 Pandemic: Filtration Efficacy and Air Resistance. *J Aerosol Med Pulm Drug Deliv*. 2021;**34**(1):11-9.
36. Malenovska H. Coronavirus Persistence on a Plastic Carrier Under Refrigeration Conditions and Its Reduction Using Wet Wiping Technique, with Respect to Food Safety. *Food Environ Virol*. 2020;**12**(4):361-6.
37. Grove SF, Lee A, Lewis T, Stewart CM, Chen H, Hoover DG. Inactivation of foodborne viruses of significance by high pressure and other processes. *J Food Prot*. 2006;**69**(4):957-68.
38. Liu P, Yuen Y, Hsiao HM, Jaykus LA, Moe C. Effectiveness of liquid soap and hand sanitizer against Norwalk virus on contaminated hands. *Applied and Environmental Microbiology*. 2010;**76**(2):394-9.
39. Bouwknegt M, Verhaelen K, Rzetutka A, Kozyra I, Maunula L, von Bonsdorff CH, et al. Quantitative farm-to-fork risk assessment model for norovirus and hepatitis A virus in European leafy green vegetable and berry fruit supply chains. *International Journal of Food Microbiology*. 2015;**198**:50-8.
40. Bean B, Moore Bm, Sterner B, Peterson LR, Gerding DN, Balfour H. Survival of influenza viruses on environmental surfaces. *J Infect Dis*. 1982(0022-1899 (Print)).
41. Nicas M, Jones RM. Relative contributions of four exposure pathways to influenza infection risk. *Risk Anal*. 2009;**29**(9):1292-303.
42. Greene C, Vadlamudi G, Eisenberg M, Foxman B, Koopman J, Xi C. Fomite-fingerpad transfer efficiency (pick-up and deposit) of Acinetobacter baumannii—with and without a latex glove. *Am J Infect Control*. 2015;**43**(9):928-34.
43. Rusin P, Maxwell S, Gerba C. Comparative surface-to-hand and fingertip-to-mouth transfer efficiency of gram-positive bacteria, gram-negative bacteria, and phage. *J Appl Microbiol*. 2002;**93**(4):585-92.
44. Wilson AM, Reynolds KA, Sexton JD, Canales RA. Modeling Surface Disinfection Needs To Meet Microbial Risk Reduction Targets. *Appl Environ Microbiol*. 2018;**84**(18).

45. Wilson AM, Weir MH, Bloomfield SF, Scott EA, Reynolds KA. Modeling COVID-19 infection risks for a single hand-to-fomite scenario and potential risk reductions offered by surface disinfection. *Am J Infect Control*. 2020.